16B.3 EVOLUTION OF EYEWALL-LIKE, UNSTABLE VORTICITY RINGS

Wayne H. Schubert[1]* Jonathan Vigh[1], and Huiqun Wang[2]
[1]Colorado State University, Fort Collins, Colorado
[2]California Institute of Technology, Pasadena, California

In hurricane eyewalls the vertical stretching effect tends to produce an annular ring of high vorticity. If narrow enough, such vorticity rings can be very unstable. The end states of such instability can be of three types: (1) a vorticity monopole (i.e., high vorticity in the center); (2) a vortex crystal pattern (i.e., several mesovortices locked in rigid rotation); (3) a chaotic pattern of mesovortices. Which end state is observed depends on initial conditions such as ring diameter, ring width, and the magnitude of the depressed vorticity inside the ring. In order to better understand what types of flow patterns might be expected in real hurricanes, we have performed a systematic exploration of this "initial condition phase space" with a barotropic model. This study is an extension of the work of Schubert et al. (1999), Kossin and Schubert (2001), and Wang (2002).

The numerical model used in all our experiments is the f-plane version of the multigrid barotropic model (MUDBAR) developed by Fulton (2001). Using Cartesian coordinates (x, y) the governing vorticity equation and invertibility principle are

$$\frac{\partial \zeta}{\partial t} + \frac{\partial(\psi, \zeta)}{\partial(x, y)} = \nu \left(\frac{\partial^2 \zeta}{\partial x^2} + \frac{\partial^2 \zeta}{\partial y^2} \right), \qquad (1)$$

$$\frac{\partial^2 \psi}{\partial x^2} + \frac{\partial^2 \psi}{\partial y^2} = \zeta, \qquad (2)$$

where ζ is the relative vorticity, ψ the streamfunction. and ν the constant diffusion coefficient. The model domain is the square defined by $-L \le x \le L$ and $-L \le y \le L$. We focus our attention on flows involving vorticity rearrangement near the center of the model domain. For such flows the far-field circulation is unchanged from its initial axisymmetric form. In order to minimize the perturbing influence of the boundary conditions, as the boundary condition on (2) we require $\psi(x, y) = [\Gamma/(2\pi)] \ln \left[(x^2 + y^2)^{\frac{1}{2}} / L \right]$ on the boundary, where Γ is the initial far-field circulation. According to this boundary condition, $\psi = 0$ at the four boundary points $(x, y) = (L, 0), (0, L), (-L, 0), (0, -L)$, and $\psi = \Gamma \ln(2)/(4\pi)$ at the four corner points $(x, y) = (L, L), (-L, L), (-L, -L), (L, -L)$. Thus, proceeding anticlockwise around the boundary there are four boundary segments on which ψ is increasing (inflow) and four boundary segments on which ψ is decreasing (outflow). Since we must specify ζ only on inflow, the boundary condition for (1) is $\zeta(x, y) = 0$ on the inflow boundary segments. These boundary conditions for our square domain give essentially the same results as requiring $\psi = 0$ on the boundary of the circular domain with radius L. It is interesting to note that these boundary conditions allow us to use a smaller domain than is required when using the doubly-periodic boundary conditions associated with a Fourier spectral model. In the spectral model the double periodicity can induce an undesireable wavenumber four structure near the center if the domain is not large enough. On the other hand the boundary condition on ψ described above is "axisymmetric," so that, if there is an induced error in the central region due to the boundary condition, this error is in the sense of suppressing asymmetry rather than enhancing it.

The numerical model uses the 4th order Runge-Kutta scheme to advance in time and has the option of 2nd or 4th order Arakawa Jacobian to approximate the advection terms. It has multiple nests within the base grid. In this study, the simulations are run on a base domain of size 4096 km × 4096 km with 256 × 256 grid points. There are four subsequent nests within the base domain, each of which has half the domain size and mesh size of its mother domain, so that the finest mesh is 256 km × 256 km with a mesh size of 1 km. In some runs, the resolution was decreased to 128 × 128 grid points for the base domain and each of the nests.

The initial condition for these experiments is $\zeta(r, \phi, 0) = \bar{\zeta}(r) + \zeta'(r, \phi)$, where $\zeta'(r, \phi)$ is a small perturbation of an axisymmetric vorticity field $\bar{\zeta}(r)$. The axisymmetric part of the initial field consists of a vorticity ring, with zero vorticity at $r = 0$. Twenty-nine experiments have been run, with initial rings having widths $4, 8, \ldots, 116$ km. All experiments have the same far-field circulation.

*Corresponding author address: Wayne Schubert, Department of Atmospheric Science, Colorado State University, Fort Collins, CO 80523-1375; e-mail: waynes@atmos.colostate.edu

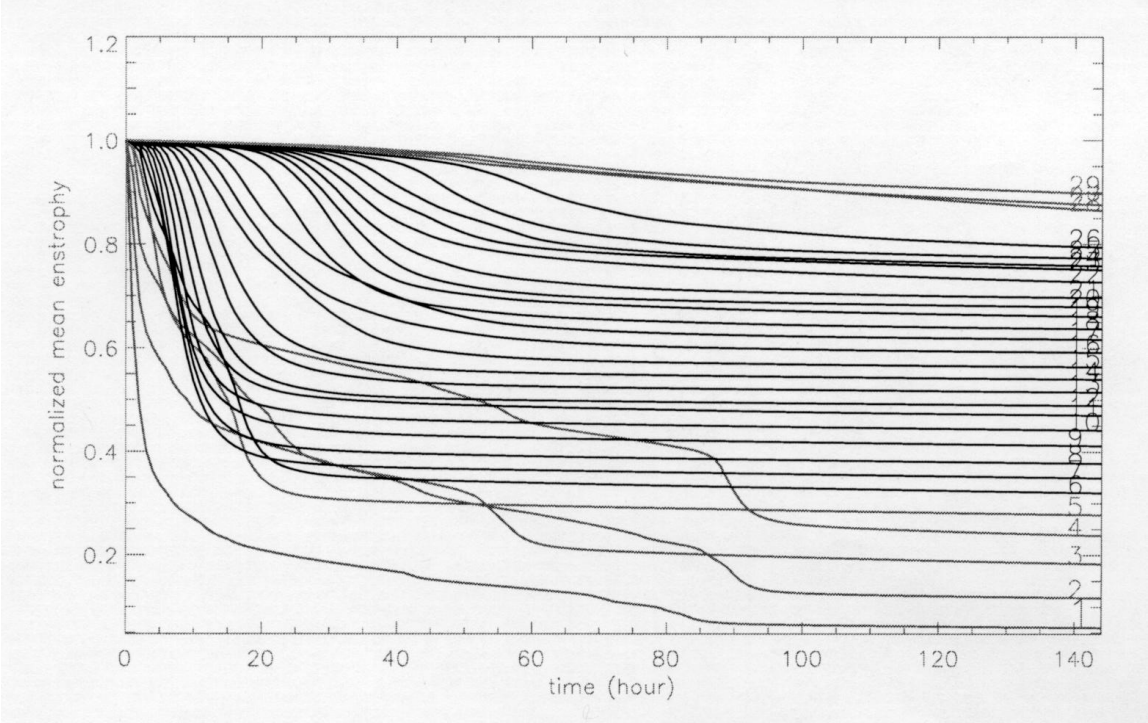

Figure 1: The normalized enstrophy $Z(t)/Z(0)$ as a function of t for 29 experiments with differing initial ring width. The initial rings have widths $4, 8, \ldots, 116$ km, and are respectively labeled $1, 2, \ldots, 29$.

The general results can be described as follows. Very wide rings (width $\geq$ 108 km) show azimuthal wavenumber 2 structures initially, but never break up into individual vortices. The central low vorticity remains for at least 80 turnaround times. Wide rings (24 $\leq$ width $\geq$ 104 km) break down into 2–5 vortices that gradually relax to a monopole. Thin rings (width $\leq$ 20 km) initially break up into many vortices ($\geq$ 6) that rapidly merge into several vortices (4–5). The resultant vortices persist for tens of rotational timescales before subsequent merger takes place. Such configurations can be referred to as "meso-vortices" or "vortex crystals."

The experiments display many of the characteristics of 2D turbulence, for example the selective decay of enstrophy over energy. As is easily derived from (1), the enstrophy evolves according to

$$\frac{dZ}{dt} = -2\nu P, \tag{3}$$

where $Z = \iint \frac{1}{2}\zeta^2 \, dxdy$ is the enstrophy and $P = \iint \frac{1}{2}\nabla\zeta \cdot \nabla\zeta \, dxdy$ is the palinstrophy. The palinstrophy, a measure of the overall vorticity gradient, can surge to very large values as the instability develops, resulting in a rapid decrease of $Z(t)$. The curves for normalized enstrophy $Z(t)/Z(0)$ as a function of t for the 29 experiments with differing initial ring width are shown in Fig. 1. The curves labeled 1, 2, 3, 4, 5 are for the thin rings with widths 4, 8, 12, 16, 20 km, and the curves labeled 27, 28, 29 are for the very wide rings with widths 108, 112, 116 km. The very thin rings show the largest enstrophy decay, but with plateaus punctuated by rapid decreases associated with the merger of mesovortices.

References

Fulton, S. R., 2001: An adaptive multigrid barotropic tropical cyclone track model. *Mon. Wea. Rev.*, **129**, 138–151.

Kossin, J. P., and W. H. Schubert, 2001: Mesovortices, polygonal flow patterns, and rapid pressure falls in hurricane-like vortices. *J. Atmos. Sci.*, **58**, 2196–2209.

Schubert, W. H., M. T. Montgomery, R. K. Taft, T. A. Guinn, S. R. Fulton, J. P. Kossin, and J. P. Edwards, 1999: Polygonal eyewalls, asymmetric eye contraction, and potential vorticity mixing in hurricanes. *J. Atmos. Sci.*, **56**, 1197–1223.

Wang, H., 2002: Rearrangement of annular rings of high vorticity. WHOI Summer Program in Geophysical Fluid Dynamics.